Optimized Off Grid Solar Charger with Dual Outputs

By

Lukas Gollings

Kanin Tangchartsiri

WonJoon Lee

Final Report for ECE 445, Senior Design, Spring 2022

TA: Akshat Sanghvi

May 4th 2022

Team 7

Abstract

The goal of this project is to design and verify the operation of a USB charger and a rechargeable battery management system, which can further extract the maximum energy from a photovoltaic source. The necessary power converter and microcontroller were developed to implement a functioning dedicated charging port for USB devices, as well as control logic for constant current charging of NiCd batteries at 70 mA. Voltage and current regulation was performed according to the IEEE code of ethics for safe battery charging. An Incremental Conductance Algorithm was researched and developed in firmware to predict the maximum power point with high precision and accelerated convergence. Applications of this device are focused on providing renewable energy to consumers, which can also be used to provide off grid charging solutions during natural disasters. The following sections elaborate on critical design decisions, design constraints, verification steps, and areas of improvement for future revisions .

Contents

1 Introduction

Nearly every city in the world is dependent on the electrical energy received from the grid. Rechargeable electronics, such as smartphones and smart batteries, are found in nearly every household; however, they must be connected to the grid each day to maintain their functionality. As people become increasingly dependent on these devices, there is an expectation that the electrical grid will be able to source power to these devices at the users convenience. The electrical grid is stable and well established in many areas, but with the increase of natural disasters associated to climate change, many people find themselves without power and having to ration the charge of their battery devices. If the grid is ever damaged and cannot be restored immediately, people are suddenly unable to communicate with emergency services using their cell phones or use battery powered radios to to receive critical information. Thus, there is a definitive need for an electrical energy source that is isolated from the grid, but is also capable of delivering power to a wide range of devices, each with different power ratings. A device that can harvest energy from a renewable source, such as a photovoltaic power source, would help provide energy when the grid is inaccessible and ensure the reliability of rechargeable electronics for these critical emergencies. Due to the inability to predict when and where a natural disaster may occur, a device that delivers power from a renewable source to small scale electronics eliminates the fear that the electronics will be unusable if the electrical grid is inaccessible.

1.1 Solution

The proposed solution to this problem consists of several subsystems working together to harvest energy from a solar panel, regulate the voltage and currents of different loads, work independently from the grid, and display the information on a user interface. These reflect the high level requirements that guided the design process. The device must source all of its power from a solar panel, including the internal power supply management and power delivered to the load(s). It should further be able to extract the maximum input power available to ensure charging speeds are fast and reliable in emergency situations. A maximum power point tracking (MPPT) algorithm can accomplish this, but additional circuitry is needed to regulate the output voltage and current to meet the power ratings of the load. Lastly, the device will display the total energy harvested from the solar panel, such that the user can measure the return of investments themselves.

1.2 Overview of Functioning Prototype

The final prototype can be summarized into four subsystems: the input power subsystem, microcontroller subsystem, the user interface, and voltage and current regulation, as shown in Figure 1. The input power subsystem involves a synchronous buck converter that delivers DC power from a photovoltaic input source to a USB device. The buck converter was developed from scratch to meet the output voltage ripple tolerance for a 5 V and 2 A load, commonly seen in many 10 W chargers. A self-created synchronous buck converter was utilized because the output current needed to be probed and fed into our control feedback algorithm. As a result, it is easier, from an implementation stand point, to probe our inductor current when the buck converter is self-built. A synchronous buck converter is chosen due to its linear gain, which is ideal for a proportional integral (PI) controller. The microcontroller is a separate system, that was designed to change the duty cycle of two complimentary pulse width modulation (PWM) signals. The microcontroller is further responsible for communicating with a OLED display via I^2C protocol. The user interface involves the OLED display, which is used to display the amount of energy harvested and the current battery status. The microcontroller further works in conjunction with the voltage and current regulation subsystem, in which the microcontroller processes feedback signals of the current battery charge and the total power being harvested from the solar panel. Voltage and current is measured at the input and output of the synchronous buck, after the DC voltage and current ripple is filtered. The voltage and power regulation subsystem has further been updated to power all of the internal components included in the design.

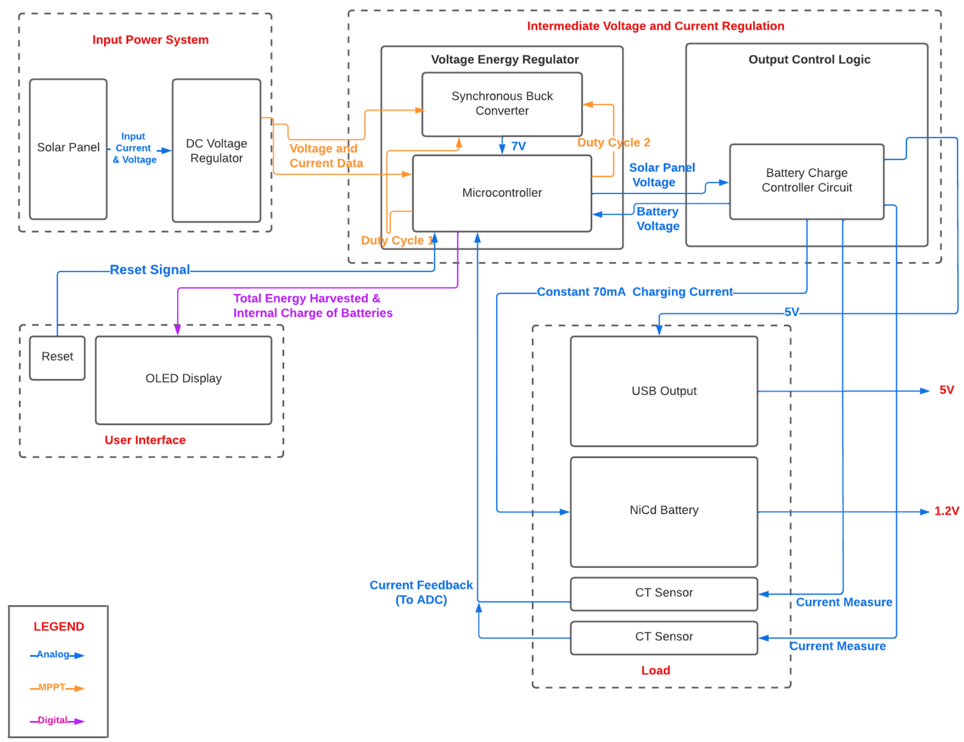

Figure 1: Block Diagram

2 Design

2.1 Input Power Subsystem

2.1.1 Synchronous Buck Converter

An extensive amount of time was spent designing the synchronous buck converter to allow us to extract power from the solar panel with high efficiency. The synchronous buck converter is able to step down the voltage of the input,given by the relationship shown in Equation 1. This topology can only step the voltage down, which is advantageous for the solar panel available in lab. The system is designed for the 100 W PV input, with $V_{OC} = 22.4V$ and $I_{SC} = 5.92A$. Note that this current is significantly large, therefore we chose to limit the the current to 3 A to avoid large trace widths and further reduce the sizing of our power electronics. The output voltage and current of the buck converter is controlled by PWM signals generated by the MCU, where D is the duty cycle. The system has been designed for a switching frequency of $f_{sw} = 100kHz$, which further affects the sizing of the inductors and capacitors (Eq 1). The output voltage and current of the synchronous buck converter will not be constant because the duty cycle will be adjusted according to the Incremental Conductance Algorithm for MPPT. The synchronous buck converter acts as a variable resistor, with minimal losses, that can adjust the amount of current drawn from the solar panel using conservation of power $P_{IN} = P_{OUT}$. The solar panel is at constant voltage, thus, as the output voltage increases with D, the input current must also increase. Hence, by applying a closed loop control algorithm to measure the output current, we can adjust the duty cycle to converge to the maximum power point. The synchronous buck converter controls the input power flow, however, there is additional filters and Linear Dropout Regulators (LDO) attached to the output to further regulate the USB charging protocol. There is still a large need to reduce the voltage and current ripple at the output so that we do not have switching noises in the DC power traces. The ripple is designed to stay within 2% of the expected V_{OUT}. Given these design constraints, the schematic of the synchronous buck converter shown in Figure 2 includes current sense amplifiers that measure the voltage across a shunt resistor. The schematic was simulated in LTSpice to further estimate the trace width and clearance between the power electronics.

Equations (1) and (2) are the input-output relationship for the buck converter. These equations determine our output voltage and current given ideal conditions with no power loss:

$$V_{out} = DV_{in} \tag{1}$$

$$I_{out} = \frac{I_{in}}{D} \tag{2}$$

where V_{out}, I_{out}, V_{in}, I_{in} are the input and output voltages and current respectively, and D is the duty cycle of our high-side MOSFET.In terms of sizing the components on the buck converter, Equation (3) determines the size of the inductor that must be utilized. The size of the inductor also depends on the switching frequency, the tolerance for our ripple current, the input voltage, and the output voltage:

$$L = \frac{V_{out}(V_{in} - V_{out})}{\Delta I_L(f_s)(V_{in})} \tag{3}$$

where L is the inductance in H, V_{out} and V_{in} is our output and input voltage respectively, ΔI_L is the inductor current ripple, and f_s is the switching frequency that drives the MOSFET [1].

Another important area to focus on is the minimum inductance to operate in continuous conduction mode for our synchronous buck which is detailed as:

$$L_{CCM} = D\frac{(V_i - V_O)R}{2fV_O} \tag{4}$$

where L_{CCM} is the minimum inductance in H, V_i is the input voltage, V_O is the output voltage, f is the switching frequency, and D is the duty cycle of the high-side switching signal [2]. It is vital that our DC-DC converter is operating in continuous conduction mode as opposed to discontinuous conduction mode.

Sizing of the output capacitors and the inductor sizing equations shares very similar characteristics. Therefore, similar conclusion can be made. The ripple voltage on both the input and output is assumed to flow through the capacitors, such that the sizing of these components are correlated with the quality of the DC output voltages. This relationship can be referenced in Equation (5).

$$C_{out,min} = \frac{\Delta I_L}{8f_s(\Delta V_{out})} \tag{5}$$

Another key aspect of the project is to choose the correct sizing for our switching MOSFETs. The MOSFETs need to be sized greater then the switch stress parameters, becasue if they are not the semiconductor will overheat and the component will break down. These can be seen through Equations (6) and (7):

$$V_{pk} = V_{in} \tag{6}$$

$$I_{pk} = (\frac{I_{L,ripple}}{2} + 1)\frac{P_{max}}{V_{out}} \tag{7}$$

where V_{pk} is the peak voltage through the MOSFET, I_{pk} is the peak current through the MOSFET, $I_{L,ripple}$ is the inductor ripple current, P_{max} is the maximum input power, V_{out} is our output voltage of the synchronous buck converter. The MOSFETs themselves need to be rated with these peak voltages and current for the worst case scenarios. For the high power operation, the MOSFET chosen for this project was IRLB8721PBF, which is rated for 30 V and 62 A [3].

The simulation referenced in figure 3 confirms the feasibility of a DC-DC buck converter system that has been cascaded with a linear dropout regulator (LDO). The LDO model used in simulation is LT1965, which is not the same as our LM317 LDO used in our project; however LT1965 has very similar capabilities, but at lower output voltages. On the graphs referenced in figure 3, it is evident that our output voltage is maintained at a constant 2.5 V which is the rated operating voltage for a LT1965. The key information that can be extrapolated from this is that a buck converter to LDO system is a viable solution to providing a USB 5 V output [4].

The simulation referenced in Figure 4 confirms the overall sizing of the components. The mathematical

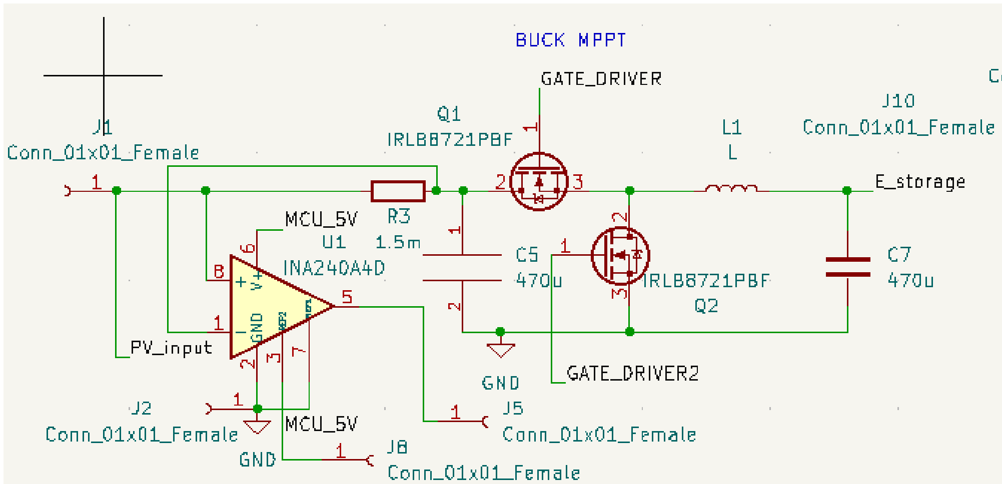

Figure 2: Synchronous Buck Converter Schematic

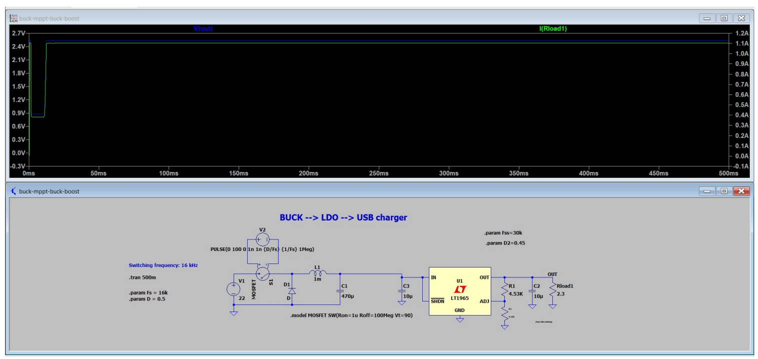

Figure 3: Buck Converter to LDO USB Charger Simulation

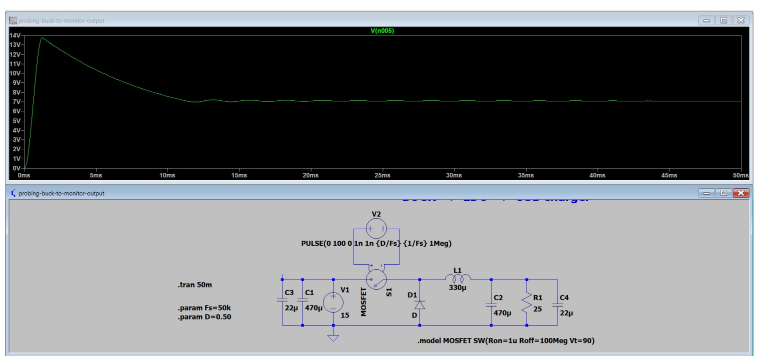

Figure 4: Buck Converter Simulation for Sizing Calculations

formulas described above are then verified in simulation, to ensure that the ripple voltage and ripple current are with their respective tolerance. It is evident from the graph itself that our synchronous buck converter operates as expected when stepping down an input of 15 V. As a result, it can be expected that with these components that our voltage out can be predicted as such.

The secondary part of the input power subsystem is designed using gate drivers and a boot strap circuit to control the switching of each MOSFET. The PWM signals cannot be applied directly to the gate of each MOSFET, due to the parasitic capacitances, C_{GS} and C_{DS}, between each pin. These parasitic elements

Parts	Size
Input Capacitance	22 μF and 470 μF
Output Capacitance	22 μF and 470 μF
Inductor	330 μH

Table 1: Component Sizing Table for Synchronous Buck Design

must be either fully charged or discharged to determine whether the MOSFET is correctly turned on or off. The gatedriver rapidly charges and discharges these capacitance, which allows the MOSFETs to be driven at higher frequencies. The LM5019 IC shown in Figue 5 accomplishes this and further ensures that the two MOSFETs are never conducting simultaneously. If the MOSFETs are both in the "on" state, the input voltage supply will be short circuited. The LM5019 further has distinct I/O pins for the high side and low side MOSFET, which allows for the designer to include a bootstrap circuit. The bootstrap circuit is needed for the high side MOSFET because V_{GS} is not equivalent to $V_G - V_S$. The PWM signal applied to each gate has an amplitude of 5V, thus, we must ensure that $V_{GS} > V_{TH}$ in order for the high side MOSFET to be on. The bootstrap circuit is designed on top of the gate driver output, which allows for our PWM signals to precisely control when each MOSFET is conducting.

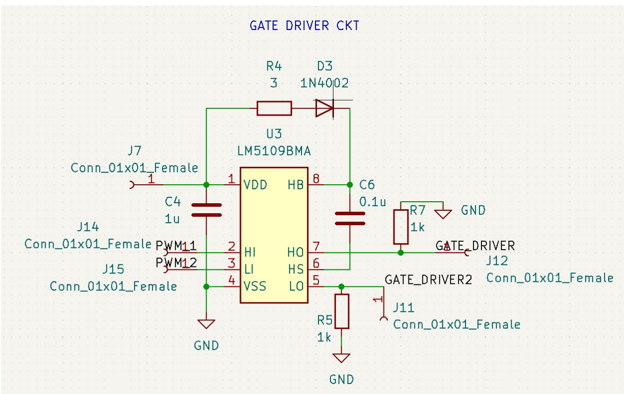

Figure 5: Gate Driver Schematic

The synchronous buck converter is the simplest DC-DC topology that will work with our MPPT algorithm. Other DC-DC topology exists, such as a buck-boost or flyback converter, but there is no situation that it is advantageous to step the output voltage to a higher potential because this will lower the input current. A DC-DC converter with galvanic isolation could be used to protect the load from unexpected faults at the input, however, this entails including a transformer in our design which will hinder our MPPT algorithm. One key advantage of the synchronous buck converter is the linear input and output relationship that is ideal for a PI controller. This linear relationship greatly improves the accuracy in tracking the maximum power point. Synchronous buck converter topology also requires a small number of components to build, hence, it was the optimal choice for our design constraints. In order to further improve on the voltage ripple of the buck, a future design may incorporate an interleaved buck converter. This converter has the same underlying principles as the synchronous buck converter, but uses several stages with a phase shift between each PWM pulse. A coupled inductor is used to deliver power to the load during each phase, which can reduce the current ripple through the inductor to allow for a better DC signal.

2.1.2 Internal Power Supply

One of the high level requirements for the project is to have the device operate entirely off-grid. More specifically, powering the MCU board to and driving the buck's gate drivers. LM317 is a three terminal linear voltage regulator that allows adjustable voltage output control. This can be controlled using an output resistor network as seen in Figure 6. Equation 8 shows the relationship between the resistor network and the output operating voltage.

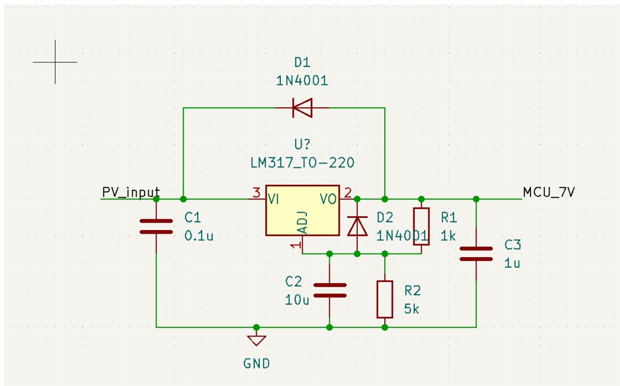

Figure 6: Internal Power Supply to MCU Board

$$V_o = V_{ref}(1 + \frac{R_2}{R_1}) + I_{adj}R_2 \tag{8}$$

where V_o is the output voltage, V_{ref} is our reference voltage, R2 and R1 are the resistors in our resistor network, and I_{adj} is the current flowing out of the ADJ terminal. The value given for V_{ref} is 1.25 V while I_{adj} is typically 50 μA. Therefore, for this particular application, I_{adj} is negligible. With the following set up referenced in figure 6, the output voltage will fall within the range of 7 - 8.5 V which will allow for the MCU board to be powered reliably utilizing only the PV input [5].

2.2 Microcontroller Subsystem

2.2.1 Design of Control Board

Another significant aspect of the design process is implementing our control system on the ATMEGA328P microcontroller as our microcontroller unit (MCU). ATMEGA328P is suitable for the design because it has three independent clocks that can generate PWM signals. It further has flexibility in setting the frequency and the duty cycle of these signals by initializing the registers with appropriate values. The MPPT algorithm is also programmed onto the ATMEGA328P, which allows us to read the analog current measurements, convert them to digital values, estimate the maximum power point, and update the duty cycle accordingly. Furthermore, the numerous I/O pins allow us to drive several other components, including NiCd battery charging logic and the I^2C LCD display. Four I/O pins are reserved exclusively for the power, SDA clock, SDA Data, and ground pins needed for I^2C communication. All of this can be done using the I/O capabilities of the ATMEGA328P, which lead the microcontroller subsystem to be centered around designing, testing, and verifying the ATMEGA328P functionality.

The MCU board has its own power system capable of outputting 5 V and 3.3 V. To output 5 V throughout the sensors and chips on the MCU board, MC33269D LDO was used. Capacitors with low equivalent series resistane (ESR) were used at the input and output of this LDO to ensure its stability. The MCU board was also designed to have the capability to shut off the 5 V supply from the USB when V_{IN} is powering the board. This logic uses a comparator that divides VIN by 2 and compares the resulting value to its 3.3 V voltage reference. The system was designed to power the entire MCU board from a 7 V to 8 V input.

2.2.2 Firmware

The firmware for this project was written in C programming language and then programmed to the ATMEGA using an external programmer. The original design of the MCU PCB also contained ICs used for USB to UART conversion to program the ATMEGA328P without an over the shelf programmer. Unfortunately, there was a significant supply shortage of these ICs, and the components needed were not available to be ordered. The solution to the supply shortage involved rerouting our pin assignments and traces to program the ATMEGA328P. An in system program (ISP) was used to burn the bootloader, and then manually convert the USB data to serial data. The over the shelf programmer used six I/O pins of the ATMEGA328, but did not effect other parts of the design.

Gate side drivers need high-frequency PWM signals to switch the buck correctly. To do this, the fast PWM capability of the ATMEGA328P was used. ATMEGA328P has a total of three pairs of fast PWM available (OC0, OC1, and OC2). Among these differently configured fast PWM pin pairs, OC2A and OC2B pins are used. These pins are able to generate complementary PWM signals of about 62 kHz, which is fast enough to accommodate the parasitic capacitance of the MOSFETs and switch MOSFETs correctly.

The aforementioned fast PWM signals were intended to be controlled using a closed loop MPPT algorithm, the incremental conductance algorithm with variable step size was chosen to allow for accurate and fast convergence to the maximum power point. The algorithm, shown in Figure 20 [6] included in Appendix C (Figure 20, calculates $\frac{dP}{dV} = 0$ in order to solve for the maximum power over any operating point. The firmware receives the current and voltage measurement using analog signals and the internal analog to digital converter. Based on the feedback signals, it predicts how far away the maximum power point, and then updates the duty cycle with a variable step size to extract additional power from the solar panel. If the operating point is close to the maximum power point, the step size is small to ensure there are no oscillations in the output. If the operating point is far from the maximum power, the duty cycle is adjusted in larger steps to accelerate convergence [6]. Ultimately, this algorithm was never fully tested on our device due to problems that arose in our power converter as discussed in Section 3.3.

2.3 Current and Voltage Regulation

2.3.1 USB Dedicated Charging Port

A synchronous buck converter for MPPT does not regulate or control the output voltage; it only can adjust the duty cycle to source more power from the solar panel. For the purpose of USB battery charging, the output potentials must be strictly regulated to ensure that the USB device is safely charging. A cascaded LDO with additional circuitry was used to regulate the output of the synchronous buck converter to be within 5 V and 2% ripple tolerance. The TPS2511 is used as a dedicated charging port, which eliminates the two data lines used for USB communication. In other words, the USB port included in our design is only capable of transmitting power and cannot send any data. The DCP is constructed by applying a constant voltage of 2 V to $D-$ and 2.7 V to $D+$ [7]. This configuration allows the external device to deliver up to 10 W of power to the load, if the load is capable of receiving this power. The TPS2511 sets the voltages off the $D-$ and $D+$, and routes the power to the peripheral USB device using the power bus [8]. The use of a DCP significantly reduces the complexity of our MPPT power supply by automating the USB charging procedure, regardless of the output voltage of our power electronics. In essence, there are two DC-DC converters cascaded in series. The first converter is the synchronous buck converter that sources power from the input solar panel, and the secondary converter further regulates the maximum power point to be within the tolerances specified for USB charging.

2.3.2 NiCd Charging

One of the requirements and verification was to have AA grade 1.2 V output storage charging available. The battery chosen for this application is a 1.2 V 700 mAh rated NiCd battery. To charge this type of battery, it is recommended to charge it with a constant current with a slow rate of charging (10 percent of the total battery capacity) for its safety and longer battery life cycle [9]. Because our application does not require any type of fast charging for the AA grade battery, a slow and constant charging mechanism was chosen. Overall, the NiCd batteries need to be charged with a fixed current, therefore charging current of 70 mA was selected as shown in Equation (9).

$$I_{Battery} = (Capacity)(0.1) = 700(0.1) = 70mA \tag{9}$$

$$I_{OperatingPoint} = \frac{V_{OUT} - V_{ADJ}}{R} = 70mA \tag{10}$$

where $I_{Battery}$ is the current flowing through battery and capacity is the total amount of energy that can be stored in the battery, $I_{operatingpoint}$ is the current flowing through the LDO, V_{OUT} is the output voltage, V_{ADJ} voltage adjust terminal.

To charge the battery with a constant current, LM317 PMIC was chosen. According to the NiCd battery charging recommendation, LM317 has been configured to output a constant 70 mA charging current by carefully tuning the component values by using the Equation (10). Below is the requirement LM317 needs to specify to operate correctly as a constant current output [10].

$$V_{Battery} + V_{Diode} + 3 \leq V_{IN} \leq V_{Battery} + V_{Diode} + 40 \tag{11}$$

where $V_{Battery}$ is the battery voltage and V_{Diode} is the current protection diode. From Equation (11), it is possible to see that depending on the VIN being provided, the amount of the battery available to charge increases. From 7 V to 8 V configured power input going into the MCU board, a maximum of about two batteries will be able to charged connected in series (to maintain 70 mA to both batteries).

To sense the battery voltage level and control the charging, the MCU reads voltage reading across the voltage divider network that ranges from 0 V to 1 V. For the analogRead() functionality, code scales this voltage reading from 0 to 1023 (at maximum). Because the maximum battery voltage is 1.25 V, charging needs to be turned off at approximately 1.2 V. For safety, the code turns off the charging enable pin when the battery voltage is at 90% (1.25 * 0.9 = 1.125 V). As shown in Figure 7, battery charging current can be turned on and off by the microcontroller PWM pins.

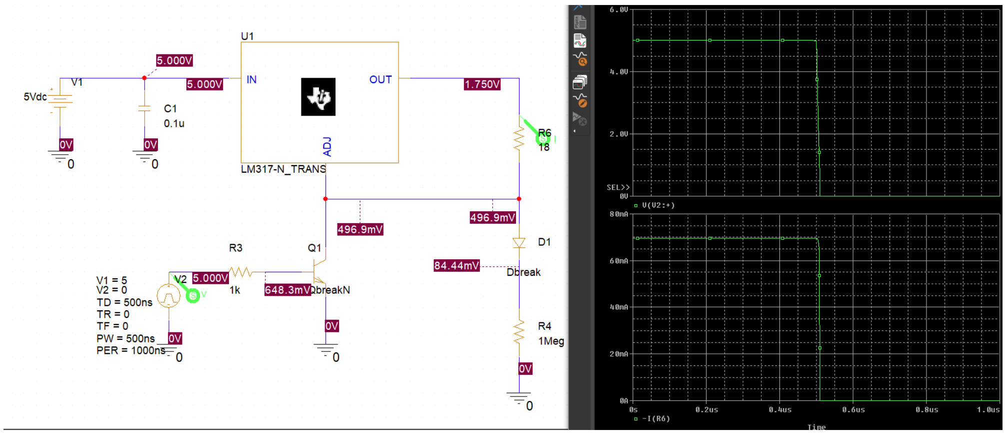

Figure 7: NiCd Battery Charging schematic and Simulation

2.4 User Interface

2.4.1 OLED Display

The OLED display must be able to accurately display the battery status and amount of energy harvested from the solar panel with high accuracy. The three signals that should be visible to the user are: charging state, battery voltage level, and total harvested energy. The battery information is critical to convey the battery charge to the user, such that they can begin using the NiCd batteries as soon as charging is complete. The total energy harvested is presented as a metric to measure the return of investments in the solar panel, if the device is used outside of natural disaster type situations. The OLED display chosen is the SSD1306 OLED Display Module, which compatible with firmware libraries compatible with the ATMEGA328P. This specific display was chosen because it uses I2C communication is used to transmit data, which only requires two I/O pins for the SDA (Data) and SCL (Clock) lines respectively but also features bidirectional communication. Data is transmitted over the SDA line, where a single bit is sent at each clock cycle. The ATMEGA328P first sends the serial address of the display and then waits to receive the acknowledge bit from the display. If an acknowledge bit is received, the host begins to transmit the data to the display to be shown. The data is transmitted synchronously with the 400 kHz SCL line, which allows for real time updates on the device operation. Ultimately, simulations could not be done in LTspice to verify the operation, however, a contingency plan was formed if the ATMEGA328P did not receive an acknowledge bit. If the microcontroller could not communicate with the display, the SDA and SCL lines could be probed with an oscilloscope to verify the display address was correct and quickly determine whether the issue was located in firmware or hardware.

3 Design Verification

As engineers, a large part of the design verification section is to probe our different output test points as outlined on the PCB schematic. Our project did not have any mechanical aspects, hence it is extremely important that the electrical characteristics of the system are thoroughly tested and documented. Individual test points are included on our PCB to allow easy access to different components of the design, where the oscilloscope could be used to debug any unexpected behavior.

3.1 Internal Power Supply to MCU Board

It is essential that the microcontroller is powered using the photovoltaic solar panel. It is evident from the Figure 8 that our MCU is receiving 7.8 V from our LDO system. This configuration allowed for a reliable power management.

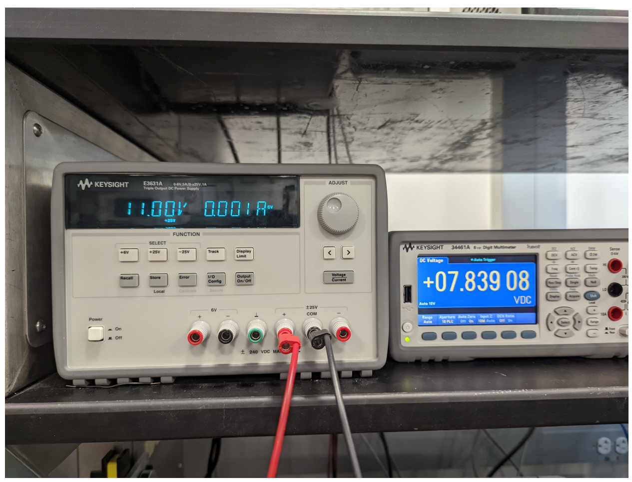

Figure 8: 7.8 V Input to MCU

3.2 Switching Signals from the Gate Drivers

Switching signals from the MCU board and the gate drivers can be seen in Figure 9. It is evident from the output of the MCU board that the PWM pins have been programmed correctly. The switching signals have been set to 62 kHz and 80 % duty cycle. It is also evident from our initial analysis of the output waveforms that our PWM switching signals from the gate drivers do possess a certain level of ringing. However, given that the current implementation requires the MCU to output our PWM, the gate driver is needed to help discharge and charge the parasitic capacitance of our MOSFETs. The ringing shown on the PWM waveform in the right is acceptable for the device operation because it mainly affects the switch stress parameters of our components.

3.3 Synchronous Buck Converter

The synchronous buck converter is another output that needs to be probed. In order to determine the characteristic of our synchronous buck converter, an input voltage sweep was performed to determine the gain. The expected gain can be determined through the formula $V_{out} = DV_{in}$ where D is the duty cycle that is utilized on the switching MOSFETs for the synchronous buck converter. The switching PWM signals' duty cycle was set to 50% and the input voltage was toggled between 0 - 20 V. When examining the differences

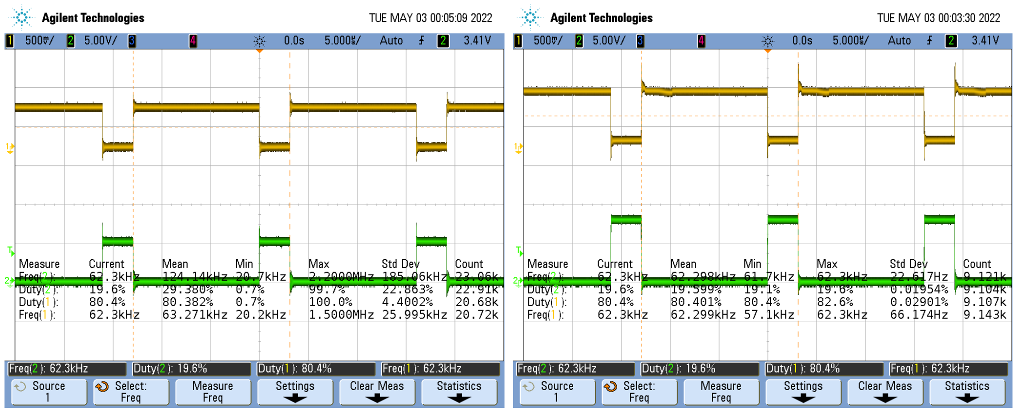

Figure 9: Switching Signal PWM from MCU Board: yellow - high side signal, green - lowside signal

between our ideal results and the output of the buck, it is evident that beyond 4.75 V input the synchronous buck converter no longer exhibits linear gain. The output of this experiment can be examined in Figure 10.

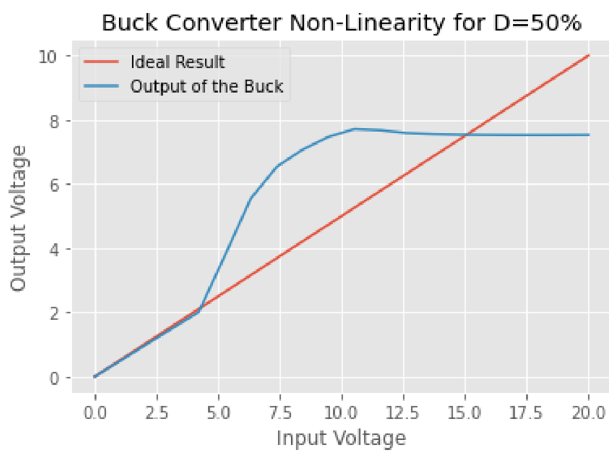

Figure 10: Plot of buck converter with sweeping input voltage

Attempts to fix the situation involved rebuilding the synchronous buck converter on a breadboard to verify the integrity of our trace signals on the PCB. This yielded no further information as to the source of the problem. Another attempt to monitor the synchronous buck converter operation was through building on a perf board. This largely yielded the same results as those from the PCB synchronous buck converter. A photo of the implementation as built on the perf board can be seen in Figure 11.

As a result of the non-linear relationship of the input and output voltage, the MPPT algorithm cannot be implemented because the feedback control requires our output relationship to be linear. However the key result to note is the operation of the buck converter at 80%. This can be referenced in Figure 12. When operating at this particular duty cycle, it is evident that the voltage plateau occurs at approximately 5 V. This is sufficient to meet our requirements and verification of outputting 5 V for our USB charging unit.

3.4 Voltage and Current Regulation of MCU

One of the most important functions of the MCU board is to output 5 V power/signals reliably because significant amount of the project's control signals and sensors depend on the 5V power source (power plane)

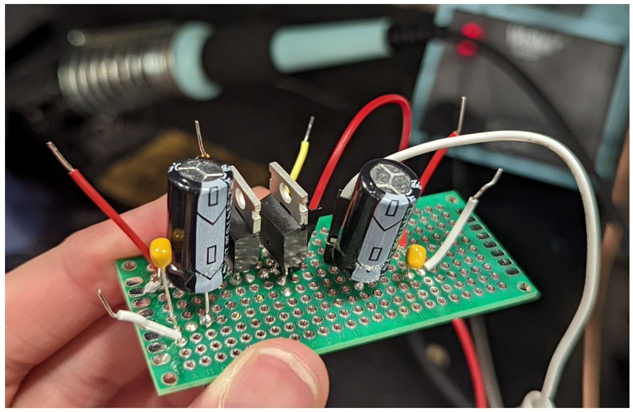

Figure 11: Perf Board Testing of the Synchronous Buck Converter

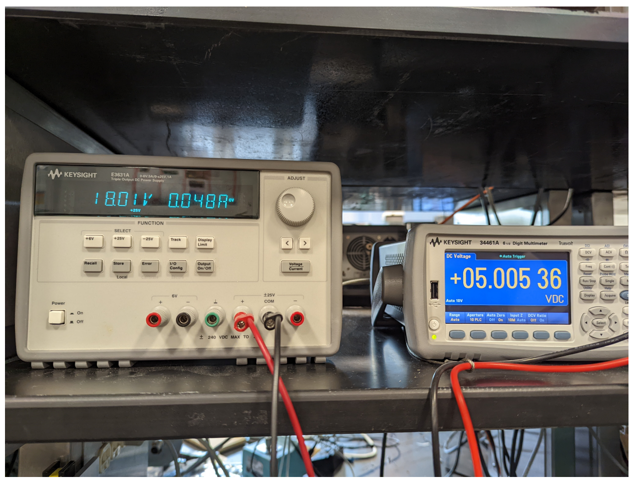

Figure 12: Output of Buck Converter at 80%

from the MCU board. To test this, one of the test point via that directly connects MC33269D's output to the PCB's power plane was probed. The result was consistent with about 5.02V, with minimized ripples. The measurement of 5V step down logic is available below in Figure 13.

Another power-related requirement that was mentioned in the requirement and verification was with the power source not interfering with the USB programming. A 3.3 V output reference voltage is created by the LP2985 fixed output LDO and an input of clean 5 V from our step-down logic. As a result, a reliable power supply using the comparator - FET power selector logic is able to reliably output a constant 5 V regardless of the input source. This value may fluctuate depending on whether the USB is powered (4.99 V with USB on and 5.02 V when V_{in} is powered). Finally, the USB debugging capability has worked in plug-and-play style regardless of the main power source coming from the input power side.

One of the main requirement and verification points of the MCU was the maximum power point tracking (MPPT) algorithm that outputs an adjustable duty cycle. However, the MPPT algorithm was not implemented due to the MPPT algorithm not being able to be performed due to the non-linearity behavior of our buck (as aforementioned in section 3.3). Instead, a manually adjustable duty cycle output code was implemented on the MCU to reliably drive our buck converter for charging purposes. The complementary duty cycle signals with a fast PWM frequency of 62 kHz of Figure 9 was generated using the OC2A and

Figure 13: PCB Power Plane and MC33269D Test Point Voltage

OC2B pins of the ATMEGA328p.

3.5 Battery Charge Controller

The most important requirement for this subsystem is a constant and consistent 70 mA current output from the battery charging circuit. With the charging from the MCU board enabled (active low), Figure 14 and Figure 15 show the current probe across the battery charging circuit with NiCd battery plugged into the load. It is possible to see when the PV modeled power source powers the power board, the current reading changes to 70.2 mA. Thus, the battery charger output functionality is well verified.

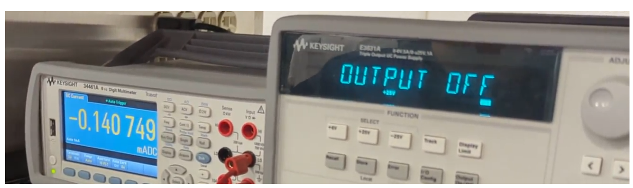

Figure 14: NiCd Charging Off State with Output Current

Another verification needed on the battery charging circuit is the charging control (enable) logic. Figure 16 demonstrates the functionality of charging control, this captures the output upon pressing the reset button of the MCU board. The reading on the multimeter verifies the functionality of our charging control logic because when the reset button is pressed for the MCU the digital output pins are set to low. However, because the battery charging circuit directly gets power from the input power of the solar panel, the overall power going into the charging circuit is not being affected. Therefore the charging enable pin is active low, which in turn provides 70 mA charging current to charge the NiCd battery. If the pin is set to high, 70 mA charging current is turned off. The same working principle is applied to the MCU programming so that when it senses the battery voltage going above 90% capacity, the enable pin is set to high to inhibit the current output.

In addition to verification of our operating voltages and currents, the temperature of operation of the LM317

Figure 15: NiCd Charging On State with Output Current

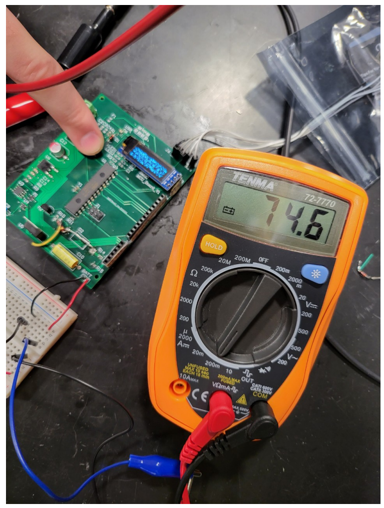

Figure 16: Reset button being pressed on MCU board - enable logic

was within tolerable conditions. The IC itself was not hot to the touch and thus it is safe to assume that it is operating within reasonable tolerances. This is also largely attributed to the fact that our operating power for the LDO is calculated to be 8.4 mW (1.2V*0.07A) which is not high power and the reference voltage (differential voltage between V_{out} and ADJ pins) is operating at the temperature sweet spot of 1.25V or below. In all, heat dissipation was not an issue for this particular subsystem.

3.6 User Interface

In the initial design considerations, it was vital that the project had a means of displaying its current charging status. Thus an OLED display was tested to see if it would accurately display battery voltage levels and charging status. Figure 17 and 18 shows how the display text is able to correctly indicate the status of our charging situation. The two situations have been recreated by 1.) feeding a 1.5 V input to simulate the no-load condition and 2.) shorting the circuit to simulate the present load condition. As evident from figures 17 and 18, our user interface has been implemented successfully and is able to correctly indicate charging status.

Figure 17: LCD display with battery charging off

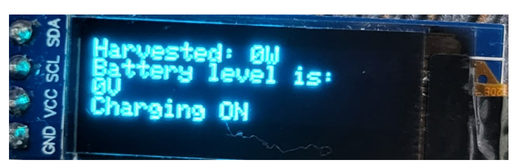

Figure 18: LCD display with battery charging on

4 Cost

One of the greatest challenges during this project was finding compatible parts during the silicon supply shortage. Many of the components needed to have sufficient voltage and current ratings for the power electronics, which significantly reduced the options when selecting capacitors and the inductor. Furthermore, many of the ICs planned to be used in the project were out of stock or were not available in the correct package. The replacements for these parts required additional components to be added to the design, which increased the cost and the size of our PCBs.

4.1 Parts

The summary of all parts used in this project is shown in Table 2. This includes a complete overview of each part that went into the final prototype model. One should note, the MCU PCB cost \$132.00 through PCBway and we had to order this PCB on our own. We were able to significantly reduce the cost, by using JLC as the manufacturer.

Table 2: Parts Costs

Part	Manufacturer	Quantity	Retail Cost (\$)	Bulk Purchase Cost (\$)	Actual Cost (\$)
PV Cell (ECEB)	n/a	n/a	n/a	n/a	0
4x1 Connector	Wurth Electrtonik	1	\$0.19	\$0.19	\$0.19
3x2 Connector	Harwin Inc.	1	\$0.29	\$0.29	\$0.29
4x1 Female Connector	Sullins Connector Solutions	1	\$0.45	\$0.45	\$0.45
6x1 Female Connector	Sullins Connector Solutions	1	\$0.52	\$0.52	\$0.52
12x1 Female Connector	Sullins Connector Solutions	1	\$0.81	\$0.81	\$0.81
ATMega328p	Microchip	1	\$5.50	\$5.50	\$5.50
Button Switch	TE Connectivity	1	\$0.04	\$0.04	\$0.04
16MHz Resonator	Murata Electronics	1	\$0.29	\$0.29	\$0.29
Battery	Panasonic BSG	2	\$2.28	\$4.56	\$4.56
1N4148	Diotec Semiconductors	1	\$0.11	\$0.11	\$0.11
0.1uF Film Capacitor	Illinois Capacitor	1	\$0.96	\$0.96	\$0.96
1N5404G	Onsemi	1	\$0.48	\$0.48	\$0.48
I2C Display	Frienda	5	\$3.60	\$3.60	\$17.99
BC547BBU	Onsemi	1	\$0.38	\$0.38	\$0.38
LM358D	Texas Instruments	1	\$1.18	\$0.82	\$1.18
LP2985IM5-3.3	Texas Instruments	1	\$1.39	\$0.69	\$1.39
LM317	Onsemi	5	\$0.83	\$0.83	\$4.15
MC33269D	Onsemi	1	\$0.78	\$0.30	\$0.78
0.01uF Cap	TDK Corporation	2	\$0.64	\$0.64	\$1.28
100pF Cap	Murata Electronics	1	\$0.38	\$0.09	\$0.38
10k Resistor	TE Connectivity	3	\$0.01	\$0.03	\$0.03
Continued on next page					

Table 2 – continued from previous page

Part	Manufacturer	Quantity	Retail Cost ($)	Bulk Purchase Cost ($)	Actual Cost ($)
10k Resistor	Yageo	2	$0.01	$0.01	$0.02
P-Channel MOSFET	Rohm Semiconductor	1	$0.45	$0.16	$0.45
3.3k Resistor	Rohm Semiconductor	1	$0.1	$0.03	$0.1
18 Ohm 1W Resistor	Vishay	1	$0.03	$0.03	$0.03
CL21B104KBCNNNC	Samsung Electromechanics	4	$0.1	$0.01	$0.4
2Pos Terminal Connector	Phoenix Contact	1	$1.21	$1.01	$1.21
10uF Cap	TDK Corporation	1	$0.28	$0.06	$0.28
120pF Cap	Kyocera AVX	1	$0.1	$0.01	$0.2
47uF Capacitor	Wurth Electronik	2	$0.32	$0.19	$0.64
5V/2A Linear Regulator	Rohm Semiconductor	1	$3.04	$1.49	$3.04
0.1uF 100V Cap	Murata Electronics	5	$0.72	$0.19	$3.60
1.5m Resistor	TE Connectivity	3	$1.04	$0.39	$3.12
1uF MLCC Cap	Kyocera	6	$0.44	$0.11	$2.64
10uF MLCC Cap	Samsung Electro-Mechanics	3	$1.17	$0.46	$3.51
LM5109	Texas Instruments	2	$1.90	$1.06	$3.80
3Pos Terminal Connector	Phoenix Contact	1	$0.70	$0.05	$0.70
USB Programmar	Moyina	1	$11.99	$11.99	$11.99
Power Board PCB	JLC PCB	5	$1.54	$1.54	$7.70
Control Board PCB	JLC PCB	5	$8.75	$8.75	$43.77
PCB Enclosure	n/a	1	$10.00	$10.00	$10.00
Total	**n/a**	**n/a**	**$65.00**	**$59.12**	**$138.96**

4.2 Labor

The cost of labor for this project can be summarized in Table 3, which also estimates the total number of hours spent working on the project. Assuming that each team member worked 12 hours a week, over 15 weeks, the total number of hours is 180 hours. The total cost of labor $40,500.00 for the entire duration of the project. A complete overview of the schedule and tasks performed on a weekly basis can be found in the Appendix C (Table 9).

Table 3: Cost of Labor

Name	Hourly Rate	Hours	Total / Person	Total *2.5
Lukas Gollings	$30.00	180	$5,400.00	$13,500.00
Kanin Tangchartsiri	$30.00	180	$5,400.00	$13,500.00
Wonjoon Lee	$30.00	180	$5,400.00	$13,500.00
Total Cost for Team				$40,500.00

5 Conclusion

5.1 Accomplishments

Overall, our project successfully met nearly all of the requirements and verification we outlined for a successful project, as seen in the appendix. The MCU PCB worked exactly as designed and was able to read current measurements, generate PWM signals, control NiCd battery charging, and communicate over I^2C protocol. The prototype does not adjust its operating point to obtain maximum power tracking, yet the power electronics are still able to transmit power from source to the load. The final prototype (right) can be seen in Figure 19 next to the theoretical concept (left) developed at the beginning of the semester. Our prototype was able to safely regulate the NiCd battery voltages given the tolerance and design constraints, however, the buck converter cannot charge USB devices at 10 W. The DCP is able to detect an external device, and source up to 500 mA of current, but we could not achieve 2 A due to the non-linearity of the synchronous buck converter. The high level requirements were achieved, for example, operating entirely off grid and battery management safety, but further testing and verification must be performed to ensure the device can operate in different ambient conditions with a photovoltaic source.

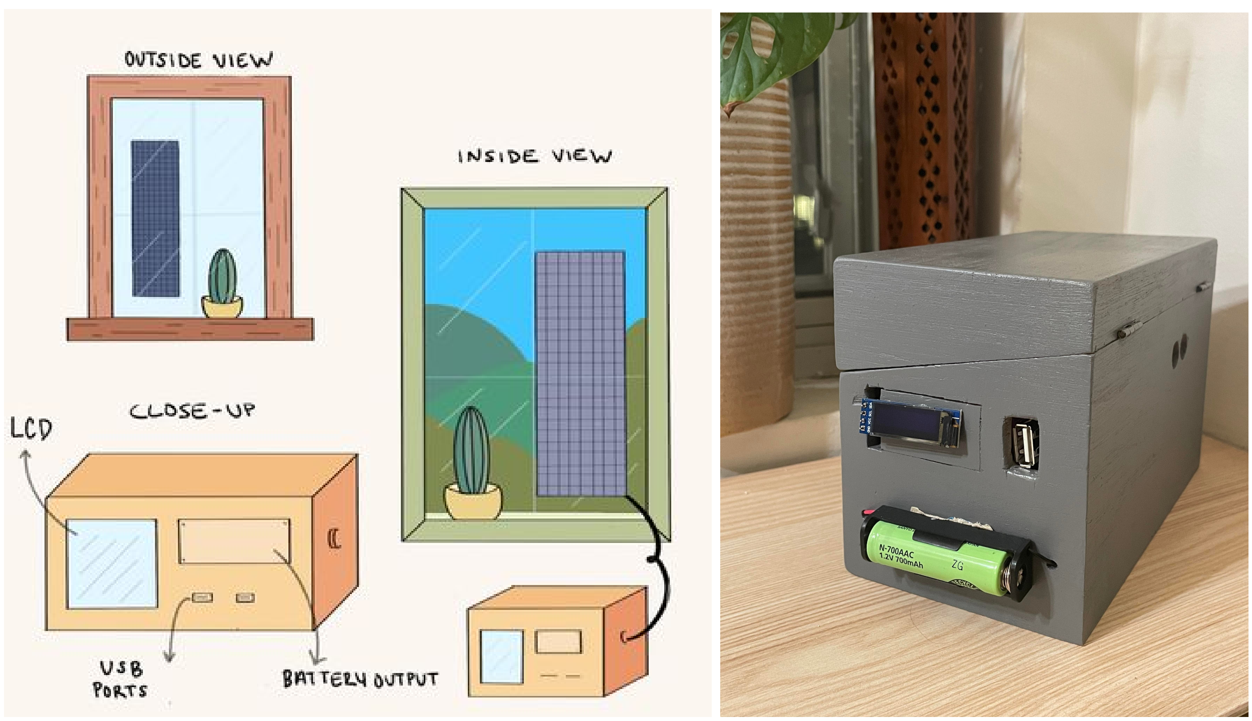

Figure 19: Proposed Design and Final Implementation

5.2 Uncertainties

Many of the unresolved aspects of our project coincide with the problems encountered verifying the operation of the synchronous buck converter. Despite the large amount of time spent troubleshooting, we were unable to obtain meaningful current measurements at the output. The microcontroller is able to read measurements at the input and output, but the analog measurements are not calibrated in the firmware. We were unable to calibrate these sensors properly due to the synchronous buck converter entering DCM and the current ripple at the output. Due to this erroneous output of the synchronous buck converter, we were unable to actively test and verify our MPPT algorithm. Another ambiguous aspect of our entire design is when there is no load attached to the solar panel. The microcontroller does not communicate with the USB DCP, instead, the TPS2511 is always powered and controls the USB power ratings. This means that we do not have any method for curtailment of the solar panel, and the prototype will still source power from the input no matter what. One solution is to attach feedback logic from the USB communication lines, such that the MCU can turn off the PWM signals when necessary and therefore stop harvesting power from the solar panel. Another possible solution is to include an energy storage unit, which redirects the power flow of there is no load attached to the device, to further improve the efficiency and available power to the user. Taking this all into consideration, we were unsatisfied with the inability to test our MPPT high level requirements and the limited power available for USB charging. These are direct consequences of the synchronous buck converter not behaving as demonstrated during the simulation, which created further uncertainties when integrating each subsystem into a single device. Future revisions to the project should focus on improving upon system integration and further analyze the tolerance of each subsystem for interconnecting components and signals.

5.3 Ethical considerations

The biggest ethical concern of our project is the safety of charging different battery chemistry's. We have made sure our device follows the documentation provided for USB charging protocol and the course policies for battery safety. It is vital to verify that the excessive strain is not being placed on our loads in order to guarantee the safety and life-span of the product. To ensure the safety of users as well as the integrity of the charging devices, it is important that all of the charging ports and units are adhering to strict charging protocol. This is mentioned within the IEEE code of conduct subsection II whereby it is paramount that individuals "treat all persons fairly and with respect, to not engage in harassment or discrimination, and to avoid injuring others". It is the responsibility of this current system to make sure that the users are kept safe and that no harm should be inflicted upon them [11].

Each member of our team conducted the battery safety training that has been provided to us by the course staff here at ECE 445. Precautionary measures have been taken to ensure the highest safety of operation, for example ensuring that we protect our system from overheating, loss of voltage and other surges that could occur while the device is operating. Furthermore, it is paramount that the sizing of our components fall within tolerable bounds to maintain integrity of our system. Extensive calculations have been made as referenced within section 2 [12].

In addition to this, as individuals who are producing this product, we have an obligation to inform the user of the most accurate information to the best of our ability. This is highlighted within the IEEE code of conduct whereby individuals should "be honest and realistic in stating claims or estimates based on available data" [11]. Most notably this is a concern when it comes to our reporting of battery levels on our LCD display. We have taken multiple measurements to verify the accuracy of our information, essentially reading the voltage levels across the batteries at different stages and calibrating our displays accordingly.

5.4 Future work

The first step that should be done to improve upon the current prototype is resolving the uncertainties of the synchronous buck converter. The unexpected non-linear behavior contradicted our reasons for choosing an incremental conduction algorithm, and ultimately we could not meet the R&V for the MPPT. Once the synchronous buck converter behaves as intended at higher voltages, we may finalize our MPPT algorithm to provide faster and more reliable charging efficiency. Furthermore, additional circuitry can be developed to improve on the design of the project. We intended to have an external energy storage unit, that controls curtailment and excess power for MPPT. This was well beyond the scope and the time frame of the project, but should be included in future versions. Other possibilities include refining our DC-DC topology selection, such as designing the system to operate at higher frequencies to reduce the size of the power electronics. There are several other step down converters that can interface with MPPT algorithms, but we suggest designing an interleaved synchronous buck converter to lower the voltage ripple at the output. The interleaved buck topology is desirable because it has the same linear gain as the synchronous buck converter, but it involves more MOSFETs that are conducting at different times for one period [13]. The PWM signals are split between several stages, which allows the user to drastically improve upon the DC voltage and reduce the switching noise observed. These features match the expected input voltage and current we designed our system around, but requires more parts and additional PWM signals which will increase the cost and complexity of the project. Nonetheless, the current prototype is far from perfect and each subsystem can be further refined in future iterations.

References

[1] B. Hauke, "Basic calculation of a buck converter's power stage," 2015, last Accessed: 2022-3-31. [Online]. Available: https://www.ti.com/lit/an/slva477b/slva477b.pdf?ts=1648604925306&ref_url=https%253A%252F%252Fwww.google.com%252F

[2] "Discontinuous conduction mode of simple converters," 2015, last accessed: 2022-5-2. [Online]. Available: https://www.allaboutcircuits.com/technical-articles/discontinuous-conduction-mode-of-simple-converters/

[3] I. Rectifier, "Irlb8721pbf," 2009, last accessed: 2022-5-2. [Online]. Available: https://www.infineon.com/dgdl/irlb8721pbf.pdf?fileId=5546d462533600a40153566056732591

[4] L. Technology, "1.1a, low noise, low dropout linear regulator," 2007, last accessed: 2022-5-2. [Online]. Available: https://www.analog.com/media/en/technical-documentation/data-sheets/1965fb.pdf

[5] T. Instruments, "Lm317 3-terminal adjustable regulator," 2020, last accessed: 2022-5-2. [Online]. Available: https://www.ti.com/lit/ds/symlink/lm317.pdf?ts=1651586740710&ref_url=%253A%252F%252Fwww.google.com%252F

[6] H.-T. Yau, Q.-C. Liang, and C.-T. Hsieh, "Maximum power point tracking and optimal li-ion battery charging control for photovoltaic charging system," *Comput. Math. Appl.*, vol. 64, no. 5, pp. 822–832, 2012.

[7] "Tps2511 usb dedicated charging port controller and current limiting power switch," 2012, last Accessed: 2022-3-31. [Online]. Available: https://www.ti.com/lit/ds/symlink/tps2511.pdf?ts=1648699644106&ref_url=https%253A%252F%252Fwww.google.com%252F

[8] R. Taylor and S. Schnier, "Creating a universal car charger for usb devices from the tps54240 and tps2511," *Texas Instrument*, 2011, last Accessed: 2022-3-31. [Online]. Available: https://www.ti.com/lit/an/slva464e/slva464e.pdf?ts=1648631024118&ref_url=https%253A%252F%252Fwww.google.com%252F

[9] "Intelligent NiCd/NiMH battery charger," last Accessed: 2022-5-4. [Online]. Available: http://electronics-diy.com/electronic_schematic.php?id=813

[10] "Lm317 3-terminal adjustable regulator," last Accessed: 2022-5-4. [Online]. Available: https://www.ti.com/lit/ds/symlink/lm317.pdf?ts=1645595845472&ref_url=https%253A%252F%252Fwww.google.com%252F

[11] IEEE, "Ieee code of ethics," 2020, last accessed: 2022-5-2. [Online]. Available: https://www.ieee.org/content/dam/ieee-org/ieee/web/org/about/corporate/ieee-code-of-ethics.pdf

[12] L. Sherman, "The basics of usb battery charging," last accessed: 2022-5-2. [Online]. Available: https://www.maximintegrated.com/en/design/technical-documents/tutorials/4/4803.html

[13] D. Baba, "Benefits of a multiphase buck converter," *Texas Instruments Incorporated*, last Accessed: 2022-3-14. [Online]. Available: https://www.ti.com/lit/an/slyt449/slyt449.pdf?ts=1648624546408&ref_url=https%253A%252F%252Fwww.google.com%252F

Appendix A Requirement and Verification Table

Table 4: R&V for Battery Charge Controller Circuit

Requirement	Verification	Y/N
1. . Battery is charged under constant current at 70mA (Charging Current = Capacity * 0.1).	1. LM317 current output should consistently be 70 mA within 10% tolerance when measured with a multimeter. 2. As long as VIN = Load voltages + 3V condition is met, constant 70 mA should be measured at the output of LM317 when measured with a multimeter.	Yes
1. According to the battery charge levels, MCU should trip or turn on the battery charging circuit.	1. When the battery level is over 95% (battery voltage of 1.2V) mark, MCU trips the charging circuitry, blocking the current flow to be around 2. If the battery charge is below 95%, MCU should turn on the charging circuitry to charge	Yes
1. LM317 operating temperature is below 125°C [8].	1. While charging the battery, monitor LM317 temperature with a thermometer. This also acts as an overall test to see if designed heat sink is doing an efficient job.	Yes

Table 5: R&V for Internal Power Management and Buck Converter

Requirement	Verification	Y/N
1. Intermediate voltages are between 7-8.5 V as input to the LDO.	1. Measure the output of the DC-DC converter to ensure the voltage stays within this range.	Yes
1. Output currents provide 2 A +/- 2% when charging.	1. Phone or device responds to the actual charging mechanism and Oscilloscope probes show 2 A average signal, using cursors to measure peak ripple.	No
1. No load conditions - If a battery is not connected, ensure $I_{out} = 0A$ and no power is drawn.	1. Connect Current probe to terminals and measure Iout. Measure the charge flowing into the battery.	Yes

Table 6: R&V for MCU

Requirement	Verification	Y/N
1. MCU is correctly being powered via VIN (internal source) and also can be debugged or programmed when the USB is plugged in. (a) Input USB devices should not power the board (FET needs to stay tripped off) when both VIN and USB are plugged in.	1. On the 5 V supply pin of the MCU, 5 V is consistently and reliably being monitored by the multimeter. 2. Switching FET gate side behavior can be monitored using a multimeter to see whether it is turned off when the VIN pin is active. 3. Uploading code to MCU should work all the time regardless of the power sources being used.	Yes
1. Based on the current measures coming from the Solar Panel, MCU outputs the correct adjustable duty cycle between 18% to 85% cycle depending on the solar irradiation.	1. Depending on the solar irradiation, duty cycle output changes and correct voltage and current can be monitored via Oscilloscope 2. Ensure that the duty cycle never exceeds 85% in peak solar insolation.	Yes

Table 7: R&V for LCD Display

Requirement	Verification	Y/N
1. I2C communication should be constantly communicating with the MCU and displaying real time data on our energy harvest (W) and battery status (%). (a) Display acts correctly as a slave and correct driven by the behavior set by SDA port of the MCU [6]. (b) Displays correct battery charging percentage in reference to 1.25 V maximum voltage rate and outputs battery percentage to the display in scale of 0 to 100%. (c) Displays total energy being harvested by solar panel in between 0 to 100 W by using MPPT algorithm data (Voltage between 0 V to 22.4 V and current between 0 A to 5.92 A).	1. When the oscilloscope is observing the SCL port during the data exchange: At the falling edge, set data bits, At the rising edge, capture data bits. 2. Battery charge level can be verified by checking if the displayed percentage is consistent with multimeter probed battery voltage. 3. Displayed wattage is consistent within 2% tolerance with the calculated via oscilloscope.	Yes

Table 8: R&V for Input Power System

Requirement	Verification	Y/N
1. Solar power can harvest a minimum of 16 W power on the weather condition in the case of high irradiation.	1. Calculate power harvested with the current and voltage data being collected via MCU and see if the power requirement is being met. Does the MCU calculations match using the oscilloscope probe?	No
1. Ensure that the MPP matches with the theoretical formula: (a) $V_{MPP} = K_V V_{oc}, 0 \leq K_V \leq 1$ (b) $I_{MPP} = K_I I_{sc}, 0 \leq K_I \leq 1$	1. Use an oscilloscope and current sensor to probe the solar panel voltage, and ensure the MPPT algorithm converges to a steady state value. 2. Probe the duty cycle with an oscilloscope and make sure it is not oscillating by more than 5%.	No

Appendix B Firmware

B.0.1 Firmware used during demo

```
#include <SPI.h>
#include <Wire.h>
#include <Adafruit_GFX.h>
#include <Adafruit_SSD1306.h>

#define OLED_RESET 4
#define buck_pwm1 5
#define buck_pwm2 6
Adafruit_SSD1306 display(OLED_RESET);
int batt_sens;
float batt_reading;

void setup() {
  display.begin(SSD1306_SWITCHCAPVCC, 0x3C);
  display.display(); //show splashscreen
  display.clearDisplay();

  pinMode(3, OUTPUT);
  pinMode(11, OUTPUT);
  TCCR2A = _BV(COM2A1) | _BV(COM2B1) | _BV(WGM21) | _BV(WGM20);
  TCCR2B = _BV(CS20);
  OCR2A = 205;
  OCR2B= 205;
  TCCR2A = 0b10110000 | (TCCR2A & 0b00001111) ;

  pinMode(buck_pwm1, OUTPUT); //PWM1 for sync buck
  pinMode(buck_pwm2, OUTPUT); //PWM2 for sync buck
  pinMode(9, OUTPUT); //batt control
  pinMode(A2, INPUT); //batt sense
  batt_sens = analogRead(A2);
  batt_reading = batt_sens * (5.0 / 1023.0);
}

void loop() {
  // put your main code here, to run repeatedly:
  //digitalWrite(3, HIGH);   // turn the LED on (HIGH is the voltage level)
  //delay(1000);             // wait for a second
  //digitalWrite(3, LOW);    // turn the LED off by making the voltage LOW
  //delay(1000);             // wait for a second
  display.clearDisplay();
```

```
  display.setTextSize(1);
  display.setTextColor(WHITE);
  display.setCursor(0,0);
  if (batt_reading < 0.95){ //battery level is below 95%
    digitalWrite(9, LOW);   // Set batt charging constant LOW (Charging)
    display.println("Battery level is: ");
    display.print(batt_reading); display.print("V");
    display.println(" ");
    display.println("Charging ON" );
  }
  else if (batt_reading >= 0.95){ //battery level is above 95%
    digitalWrite(9, HIGH);   // Set batt charging constant HIGH (Not Charging)
    display.println("Battery level is: ");
    display.print(batt_reading); display.print("V");
    display.println(" ");
    display.println("Charging OFF" );
  }
  display.display();
}
```

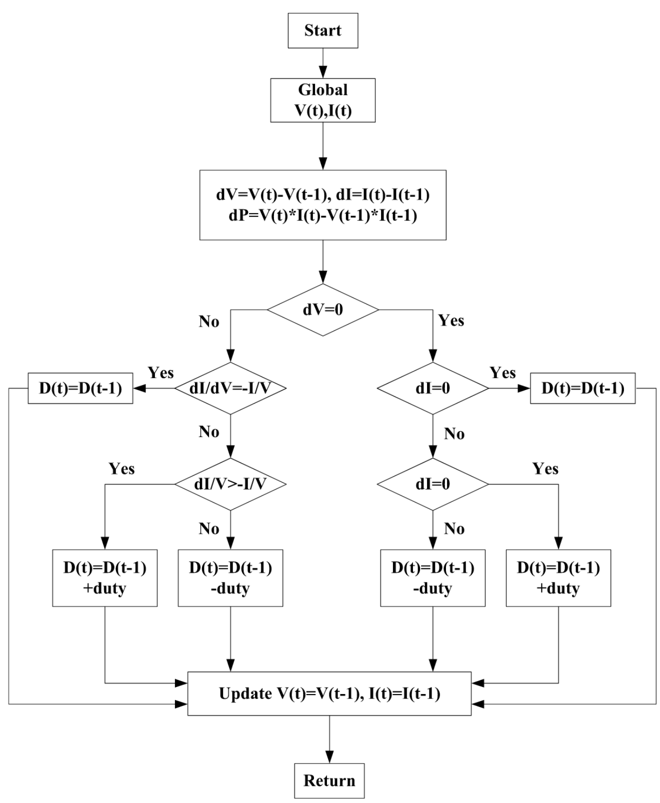

Figure 20: Flowchart of the Incremental Conduction Algorithm

Appendix C Schedule

Table 9: Schedule Throughout the Semester

Date	Lukas	Wonjoon	Kanin
2/21	1. Finish simulations of output battery terminals. 2. Finish simulations of output battery terminals. 3. Finish simulation of solar panel as input.	1. Design of MCU and necessary connections. 2. Design of analog circuit for battery management. 3. Complete the MCU Board schematic	1. MPPT simulation and design 2. Solidify implementation with regards to duty cycle control and converter topology.
2/28	1. Simulations of cascaded DC-DC converters. 2. Design Document 3. MPPT topology research	1. Finish the board layout of the MCU board 2. Pick out some parts for the MCU board	1. Simulations of cascaded DC-DC converters. 2. MPPT topology research
3/7	1. Start working on the Power Board schematic 2. Buck topology research and simulation	1. Order the MCU board 2. Make edits on the MCU board components and place an order	1. Start working on power board schematic 2. Buck topology research and simulation
3/14	1. Spring Break	1. Spring Break	1. Spring Break
3/21	1. USB A charging mechanism research 2. USB charging schematic 3. Buck converter MPPT schematic	1. Work on basic MCU board codes (I2C and Battery sensing) 2. COVID Quarantine	1. 7V internal PSU research and design 2. USB charging schematic 3. Buck converter MPPT schematic

3/28	1. Finish PCB layout of the Power Board 2. Order the Power Board parts 3. MCU Programming	1. Help Kanin and Lukas on finalizing the Power Board PCB layout 2. Start the MCU board assembly	1. Finish PCB layout of the power board 2. Order the Power Board parts 3. Order the Power Board after necessary edits
4/4	1. Pick up the Power Board PCB and start the assembly	1. Finish assembling the MCU board 2. Start testing the functionalities of the MCU board	1. Start the Power Board assembly
4/11	1. Finish assembling the power board 2. Start testing the Power Board	1. Finish testing and debugging of the MCU board 2. Finish MCU code	1. Finish the Power Board assembly 2. COVID Quarantine
4/18	1. Final Debugging plus Organize presentation 2. Debug the Buck converter 3. Rest for broken wrist	1. Debug the battery charging circuit	1. 7V internal PSU debugging 2. Buck converter debugging and editing the circuit 3. Buck prototyping on the perf board
4/25	1. MCU board PWM generation code 2. Rehearse demo	1. Finalize the MCU code and test the integration 2. Rehearse demo	1. Board integrations and testing 2. Rehearse demo
5/2	1. Practice Presentation and Finish Final Report	1. Practice Presentation and Finish Final Report	1. Practice Presentation and Finish Final Report

Appendix D Images

D.0.1 Design Figures

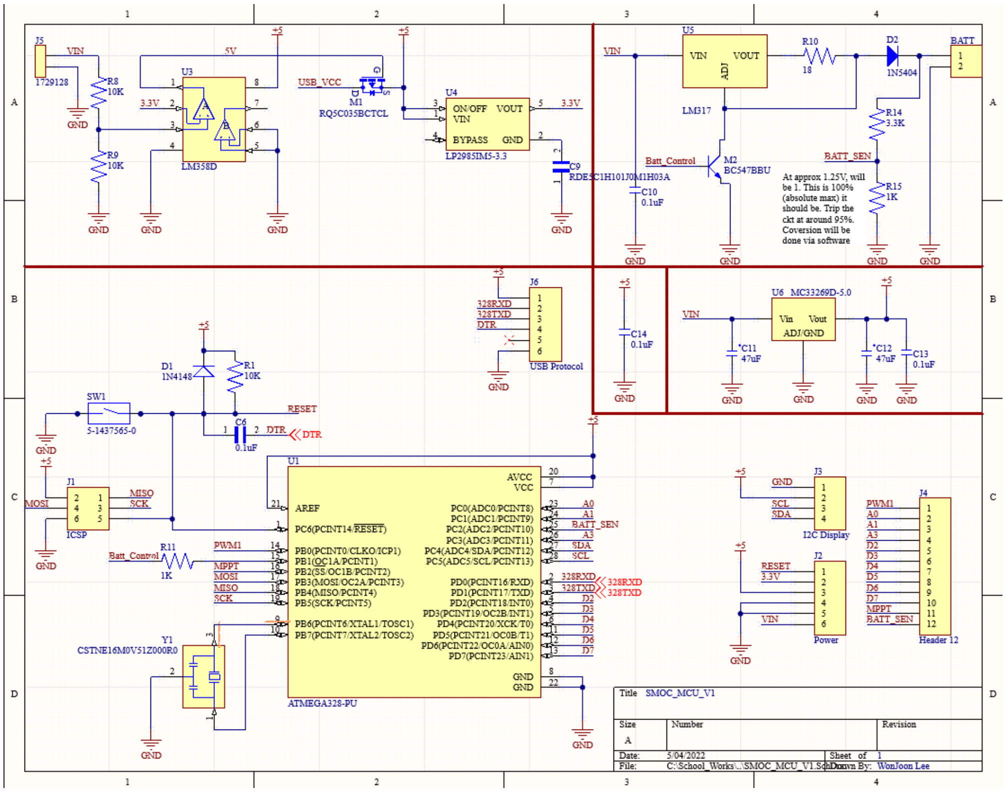

Figure 21: Schematic Of MCU Board

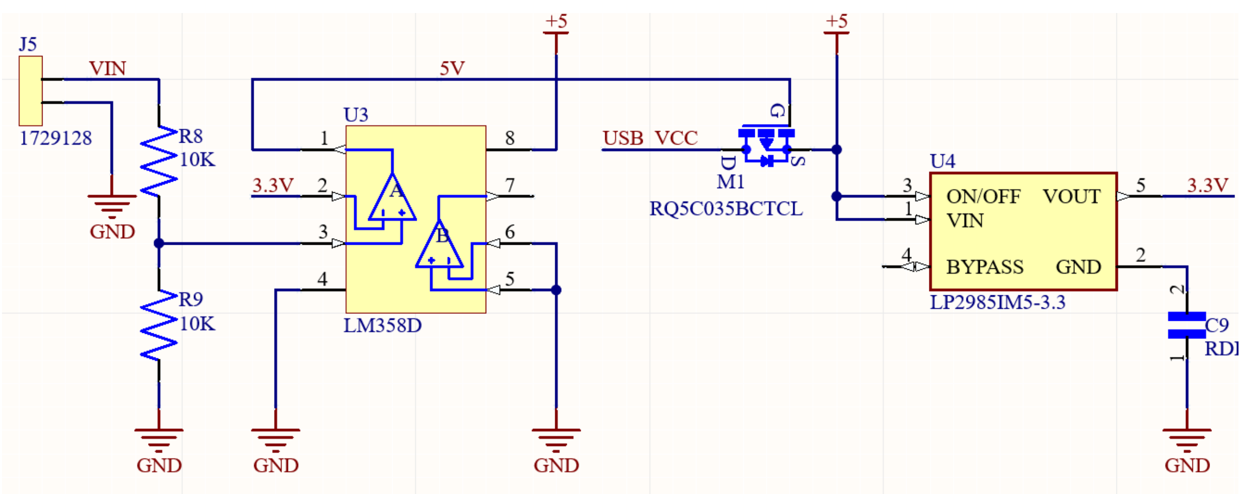

Figure 22: Schematic of Output NiCd Comparator Logic

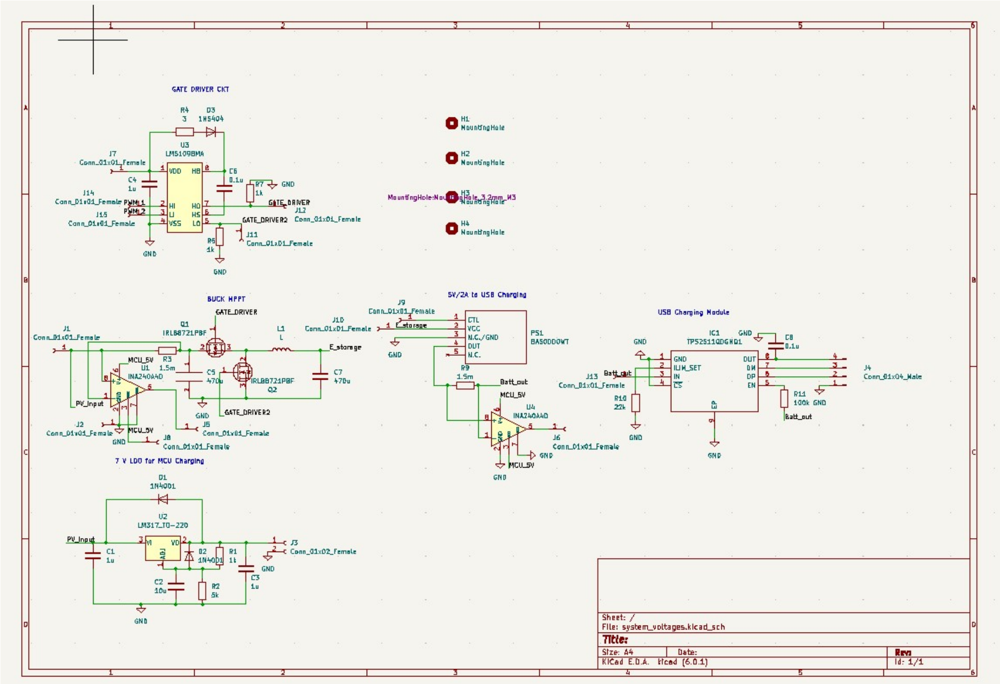

Figure 23: Schematic Of Power Board

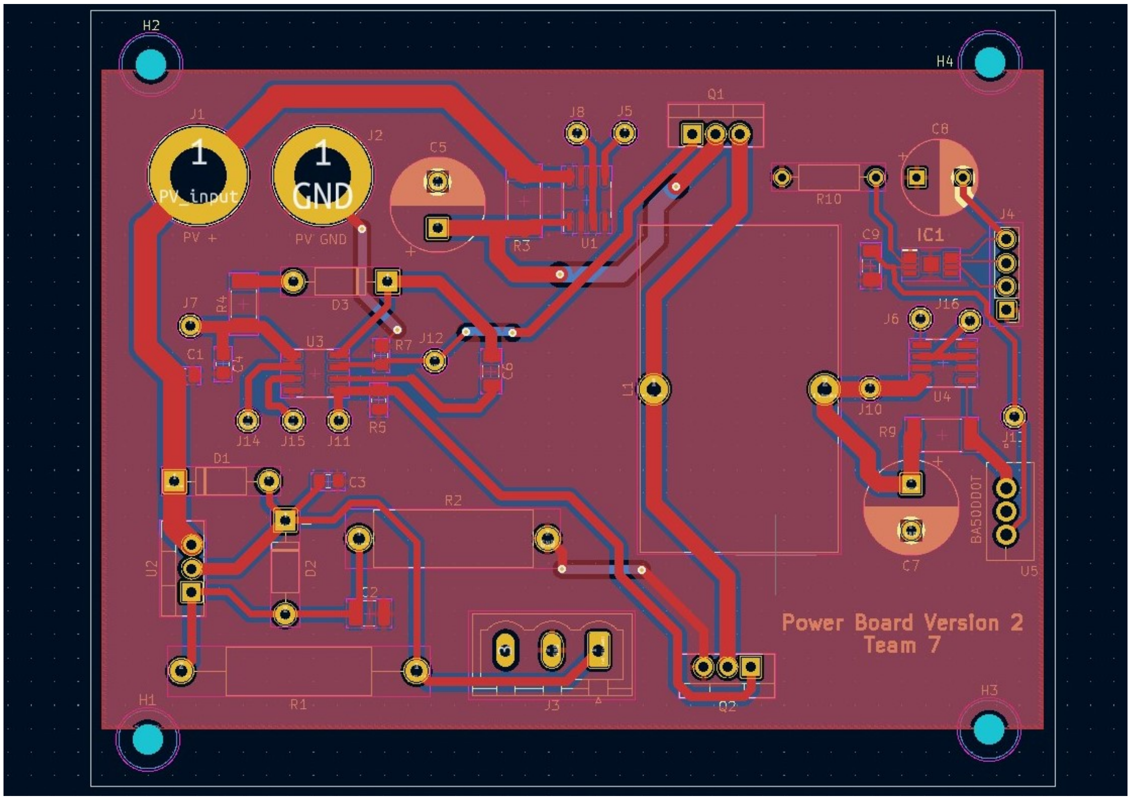

Figure 24: Final Version of Powerboard PCB

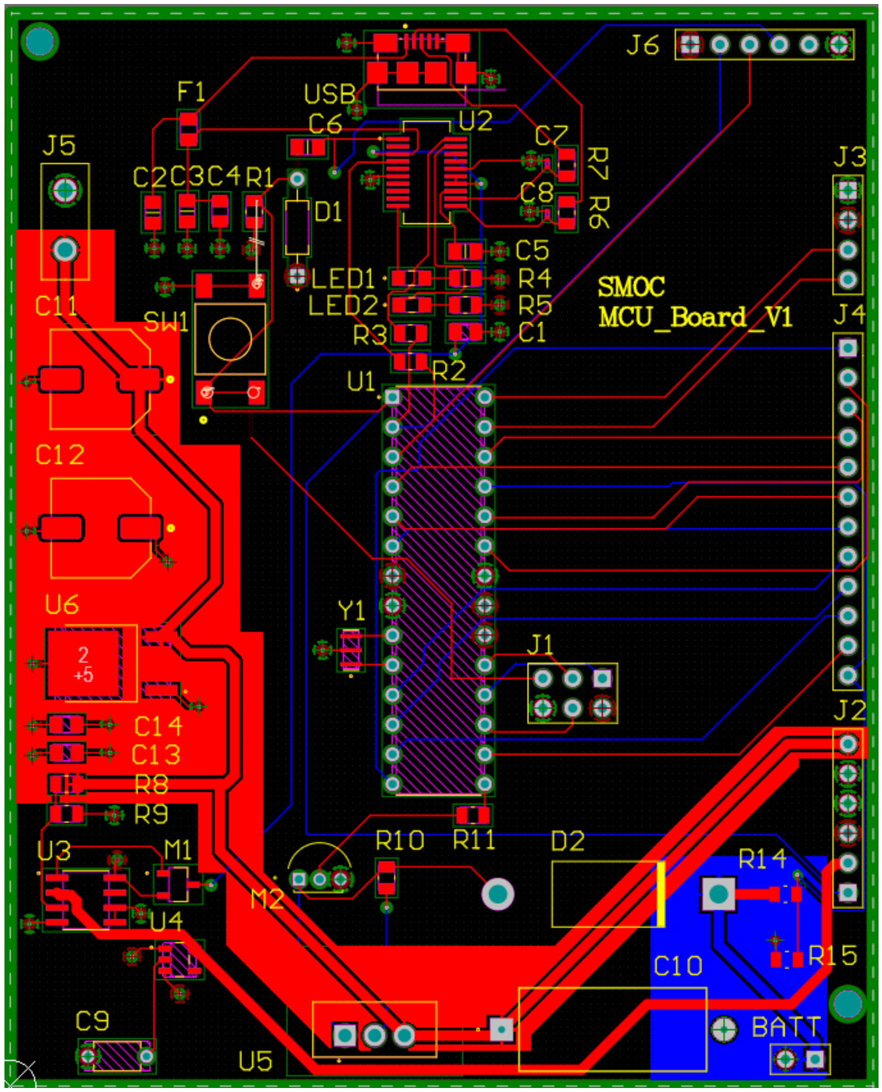

Figure 25: Final Version of MCU PCB

D.0.2 Verification Figures

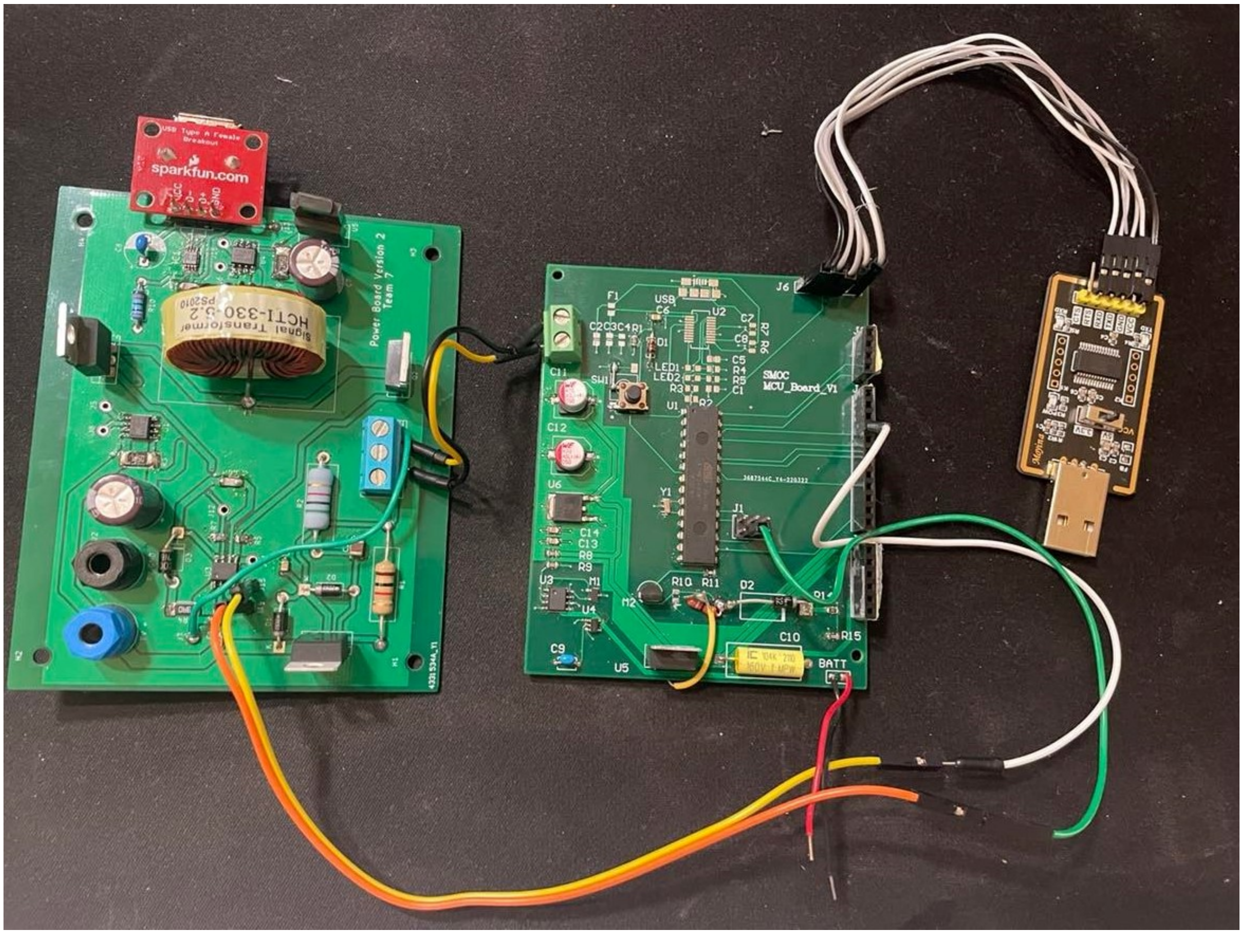

Figure 26: Close Up of PCB assembled